J. Fluid Mech. (1969), *vol.* 38, *part* 3, *pp.* 513–535
Printed in Great Britain

Reacting flow as an example of a boundary layer under singular external conditions

By RAUL CONTI AND MILTON VAN DYKE†
Lockheed Palo Alto Research Laboratory, Palo Alto, California

(Received 27 January 1969)

An inviscid flow with infinite gradients at the wall poses a problem for the accompanying boundary layer that is fundamentally different from the conventional one of bounded gradients. It turns out that in both cases the external gradients do not affect the first-order boundary layer, but the unbounded gradients generate second-order corrections that are of a lower order in Reynolds number than the conventional ones. The present singularity in stagnation-point reacting flow is of an algebraic type, and the boundary-layer corrections that it generates are proportional to non-integral powers of the Reynolds number, with exponents that vanish with the rate of reaction. The present example clarifies such matters as the matching of boundary layer and singular inviscid flow, the structure and decay of the new corrections, and their ranking in comparison with the conventional second-order effects. Numerical computations illustrate the problem and give quantitative results in a few selected cases.

1. Introduction

Boundary-layer theory was developed to deal with thin regions of a flow (usually along a boundary), where some of the flow properties sustain drastic changes in the normal direction. In fact, one of the basic ideas involved in the theory is that normal gradients in the boundary layer are large compared with those in the inviscid flow. The present paper deals with a case where this relationship is by necessity violated, since the inviscid gradients are unbounded near the wall. In the present case, this situation arises when a slowly reacting inviscid flow approaches a stagnation point, where the lagging reactions start dominating the flow and drive it to equilibrium in a final burst involving infinite gradients of temperature, density, and concentration.

The concept of a boundary layer was formulated by Prandtl in connexion with flow over a flat plate. In that case, the inviscid flow is uniform so that external gradients are absent. In the ensuing applications the theory proved successful in cases where external gradients exist but are bounded, at least near the boundary in question. In such cases the validity of boundary-layer theory can be supported from the point of view that Prandtl's theory is the first in a system of approximations that describe the flow *asymptotically* as the Reynolds number approaches infinity. In this view, any bounded external gradient is rendered

† Also, Department of Aeronautics and Astronautics, Stanford University, Stanford, California.

small in comparison with boundary-layer gradients, which become asymptotically large with the Reynolds number. Thus, if the Reynolds number is large enough, the situation reverts to Prandtl's. However, it is clear that unbounded external gradients cannot be similarly dismissed. It follows that an important distinction of principle must be drawn between unbounded external gradients and bounded ones, however large these may be. If the inviscid flow exhibits unbounded gradients at the wall, the applicability of boundary-layer theory is questionable, and it is not clear how the matching of boundary layer and inviscid flow will be accomplished.

The presence of singularities in inviscid flows has been pointed out sporadically by different authors, but perhaps the first systematic treatment of a boundary layer under a singular inviscid flow is due to Burggraf (1966), who investigated radiating flow near a stagnation point in a transparent medium. Under these conditions the inviscid flow has a logarithmic singularity at the stagnation point, and the author constructed a boundary layer that matches that behaviour. This is not a conventional boundary layer though, since its thickness is a complicated function of the Reynolds number (involving a logarithm) rather than the familiar square root. Unfortunately, it turns out that this is a degenerate case that occurs when the wall enthalpy is a vanishing quantity related to the small parameter. If one reworks the problem retaining a fixed wall enthalpy of order unity the conventional boundary layer re-emerges, and the exotic effects are relegated to higher-order approximations. The same pattern appears in the present example where, in spite of an external singularity, Prandtl's boundary layer is still the appropriate first approximation, but new higher-order effects come into play. The asymptotic expansion describing the flow in the boundary layer does not proceed in the usual negative half-powers of the Reynolds number, but in more general fractional powers that depend upon other parameters in the problem. Thus, in a slowly reacting flow a number of such terms take precedence over the conventional second-order boundary layer. This, of course, upsets the order of the error that one has come to expect of boundary-layer theory.

Two recent works where singularities appear in the inviscid flow share some of the characteristics described above. Lee & Cheng (1969) studied hypersonic flow in the 'strong interaction' régime, where the boundary layer itself forces non-uniformities into the inviscid flow. They formulated the problem in terms of a viscous layer, an inviscid external flow, and an intermediate layer. The first-order boundary layer is the conventional one, but new second-order effects appear. Similar features are present in the work of Hersh (1968), who considered rotational flow near a three-dimensional stagnation point. There the singularity is connected with the stretching of vortex tubes in the vicinity of the wall. The second-order problem is not actually solved, but the existence of the solution is inferred on the grounds of being needed to match the external flow.

In the present work, as well as in Lee & Cheng's and Hersh's, the singularities appearing in the inviscid flow are of an algebraic form involving fractional or irrational powers of the distance to the wall. These singular flows generate second- and higher-order boundary layers having algebraic behaviour at large distances from the wall. In particular, this involves an algebraic decrease of vorticity. (We shall retain the word 'decrease' to denote the behaviour in the boundary layer, and make a distinction with 'decay', which involves a comparison with the level of vorticity in the outer flow.) The algebraic decrease is not discussed by Lee & Cheng, but is noted by Hersh, who concludes that there is an algebraic *decay* of vorticity, and as a consequence the new effects in fact outreach (by an order of magnitude) the conventional boundary layer, which decays exponentially. This conclusion is not supported by the present work. Boundary-layer phenomena have long been associated with exponential decay of vorticity, and the present investigation gives no reason to believe otherwise. The key question concerns the correct level from which the decay of vorticity should be measured. In the present case the algebraic decrease of vorticity in the second-order boundary layer precisely matches a corresponding behaviour in the second-order outer flow (the flow due to displacement thickness, not investigated by Hersh). As a result the difference between boundary-layer and outer vorticity, when carried out to second order in the outer flow, does not contribute to an algebraic decay. If this extends to higher orders, as is likely, the exponential decay of the conventional boundary layer prevails, and the boundary-layer flow does not outreach itself through higher-order effects.

A difficulty associated with the external singularity that is either absent or goes unnoticed in other works arises in the construction of uniformly valid solutions. The present investigation shows that if the external singularity is described asymptotically near the wall by a single algebraic term, then a single higher-order approximation in the boundary layer will remove the singularity, and a uniformly valid composite solution can be constructed in the usual way. Similarly, if the inviscid flow contains several singular terms, an equal number of higher-order approximations is needed to remove the singularity completely. If the available higher-order solutions are outnumbered by the singular terms (as in the present case), the composite solution or some of its derivatives will be singular at the wall. Thus, one can find oneself in the position of having outer and inner solutions valid to a certain order, but lacking a systematic way to combine them into a composite solution that is free of singularities in all of its derivatives.

One of the reasons for undertaking the present investigation was to assess the current engineering practice of 'edge patching'. This practice in effect ignores the singularity in the inviscid flow on the grounds that it will be buried in the boundary layer. The neighbourhood of the singularity is bridged simply by patching the boundary layer to the inviscid flow at some point beyond the singularity, where the edge of the boundary layer is estimated to be. This procedure cannot be systematically improved, and therefore the order of the error involved cannot be estimated from within. Comparison with the present results shows that patching at the physical edge of the boundary layer can give substantial errors, but smaller errors arise from patching at the displacement edge, and this last procedure may be acceptable for ordinary applications.

In the following sections we will develop in increasing detail the ideas already discussed.

2. Analysis

General remarks and assumptions

Reacting flow near a blunt stagnation point provides a good example to test boundary-layer theory in the presence of a singular inviscid flow, since the singularity involved is of a general algebraic type with variable exponent. Thus, one can study the effects of the singularity as the exponent varies from zero to infinity, and we shall see that the magnitude of the exponent determines whether those effects are larger or smaller than the conventional second-order corrections. From a physical standpoint, the inviscid singularity arises from the inability of the reacting flow to accommodate immediately to changing local conditions. Thus, the flow may reach the vicinity of the stagnation point substantially out of chemical equilibrium, but since the point itself is in equilibrium, the stagnation neighbourhood will sustain large thermodynamic gradients. This situation is more pronounced in slowly reacting flows, which may derive from small reaction rates, low density, small body dimensions, or high flow speed. In any case, the slowly reacting inviscid flow struggles to reach equilibrium within a small region, and in the absence of dissipative mechanisms to check the steepening of gradients, these become unbounded near the wall. We will see that rapidly reacting flows have zero gradients at the wall, but the singularity is still present in some higher derivative as long as the flow falls short of complete equilibrium.

In order to study the interaction of boundary layers and singular inviscid flows, we shall strip the problem of as many complicating features as possible. To this effect, we adopt the ideal dissociating gas (Lighthill 1957), which is one of the simplest models in general use for the common atmospheric gases. The molecular-transport effects that generate viscosity, heat conduction, and diffusion are assumed to be such that the Prandtl and Lewis numbers are unity and the coefficient of viscosity is constant. It is presently known that the coefficient of viscosity and the Lewis number may vary substantially in the flow field, and engineering applications may require that this be accounted for. In particular, the 'compressibility transformation' and similar techniques are available to relax the restrictions, but we ignore such refinements in the name of simplicity. As a consequence, we shall spend no effort in trying to correlate present numerical results with available data; instead, we shall concentrate on the basic questions of applicability of the boundary-layer concept, matching with the inviscid flow, order of the error involved, and the like.

We will make a further assumption that bears some discussion. The present problem involves a chemical length and a viscous length, and one can consider different asymptotic limits depending on which one vanishes faster. In fact, the more realistic problem may be one where these lengths retain a fixed ratio, but we investigate here the case of small viscous length (large Reynolds number) with fixed chemical length. Thus, we regard the present problem as an extension of the classical boundary-layer theory, which applies when the viscous length is small compared with other lengths in the problem. As in the classical case, we will compute numerical examples for finite values of the Reynolds number (and chemical parameter), but the reader is reminded of the special nature of the present asymptotic limit.

We will cast the problem in the form of matched asymptotic expansions, as described by Van Dyke (1964). The details concerning dimensionless variables, differential equations, boundary and symmetry conditions, and the choice of co-ordinate system, are found in the appendix. The co-ordinates are shown in figure 1.

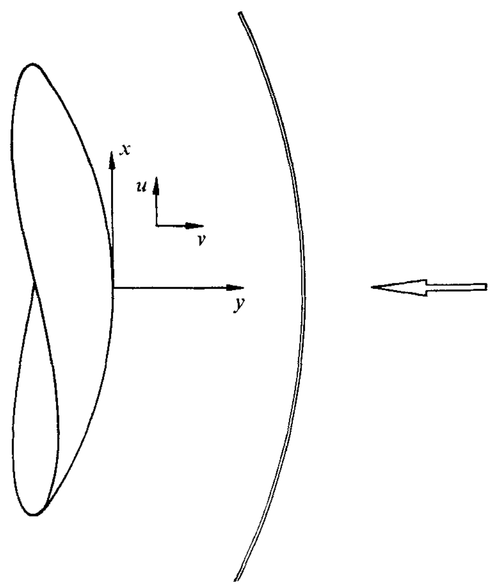

FIGURE 1. Co-ordinate system and velocity components.

The outer expansion

We are interested in a small neighbourhood of the stagnation streamline, and therefore we expand each flow variable (according to its symmetry) in even or odd powers of the co-ordinate x, and retain only the first term of the series. In addition, we re-expand this term for large Reynolds number. In this second expansion the leading term represents the inviscid flow, and we assume on a trial basis that the secondary term represents the flow due to displacement thickness, and is proportional to the inverse square root of the Reynolds number as in the conventional case. It follows that the outer expansion for, say, the degree of dissociation is

$$\alpha(x,y;\,R) = \alpha_1(y) + \frac{1}{R^{\frac{1}{2}}}\alpha_2(y)\ldots + O(x^2). \tag{1}$$

Expansions for the other variables are found in the appendix (equations A 2). Substitution of the outer expansions into the governing Navier–Stokes equations (A 1) yields the ordinary differential equations for the first-order problem (A 3) and the second-order problem (A 4). The corresponding boundary conditions are obtained by similar substitutions. With the problem cast in this form, we abandon the x-dependence of the flow variables and work with functions of y alone that represent the flow in a small neighbourhood of the stagnation streamline.

The first-order outer problem

This problem, governed by equations (A 3), describes the inviscid flow and has been solved by Conti & Van Dyke (1969). In this section we discuss the main results of that work. A complete solution is available in numerical form, and an asymptotic solution for $y \to 0$ is available in analytical form. For present purposes we concentrate on the latter, which is needed to match the inviscid flow to the boundary layer. The asymptotic solution shows that in some neighbourhood of the stagnation point ($y = 0$) the inviscid flow is described by series in positive powers of y, containing both integral and non-integral powers. The integral powers are the same that appear in inert flows. The non-integral powers are associated with the chemical reactions, and contain a reaction parameter having the form of the Damköhler number. The general term of the series is of the form y^{m+nK}, where m and n are positive integers or zero, and the reaction parameter K is

$$K = \frac{1/A}{\tau_0}\left\{1-\frac{1-\alpha_0}{2-\alpha_0}\left[\frac{\alpha_0}{1+\alpha_0}-\frac{\alpha_0}{4+\alpha_0}\left(1+\frac{\theta}{T_0}\right)^2\right]\right\}.$$

Here $\tau_0 = [\rho_d(1-\alpha_0)]/[\Gamma\rho_0^2\alpha_0(2-\alpha_0)]$ is the chemical relaxation time at the stagnation point, and $1/A$ is the flow time, related to the velocity gradient at the stagnation point by $A = (j+1)\,(\partial u/\partial x)_0 = -(\partial v/\partial y)_0$. The reaction parameter K ranges from zero in frozen flow to infinity in equilibrium flow.

It is clear that the presence of non-integral powers makes every flow variable singular to some degree, but some variables are less affected than others. Thus, the normal velocity and the variations in pressure and enthalpy retain to lowest order the same behaviour as in the inert flow; that is,

$$v_1 = Ay + O(y^{1+K}), \tag{2a}$$

$$p_1 = p_0 - \tfrac{1}{2}\rho_0 A^2 y^2 + O(y^{2+K}), \tag{2b}$$

$$h_1 = h_0 - \tfrac{1}{2}A^2 y^2 + O(y^{2+K}). \tag{2c}$$

On the other hand, the tangential velocity, temperature, density, and degree of dissociation, which share a common behaviour, may depart significantly from the inert flow, depending on the value of K. These variables are described by series of the form

$$\alpha_1 - \alpha_0 = B_1 y^2 + B_2 y^3 + \ldots + C_1 y^K + C_2 y^{2K} + \ldots + D_1 y^{1+K} + D_2 y^{1+2K} + \ldots, \tag{2d}$$

where B_i, C_i, D_i are constants. For $K > 2$ the leading term is the quadratic one (as in the inert flow), but for $K < 2$ one or more non-integral powers take precedence. In fact, as $K \to 0$ an unbounded number of such terms will precede the integral powers. We note that the case $K = 1$ is a divide between slowly reacting flows ($0 < K < 1$), which approach the stagnation point with unbounded gradients proportional to y^{K-1}, and rapidly reacting flows ($1 < K \leqslant \infty$), which approach with vanishing gradients. The singularity is then stronger in the slowly reacting flows, where it affects the first derivative, than in the rapidly reacting flows, where it affects a higher derivative. For this reason we adopt the slowly reacting flows as the basis for our present study. For $K < 1$, Conti & Van Dyke

(1969) have solved for the leading terms of the series. In present notation, the results are:

$$\alpha_1 = \alpha_0 + C_\alpha y^K, \tag{2e}$$

$$u_1 = A + C_u y^K, \tag{2f}$$

$$\rho_1 = \rho_0 + C_\rho y^K, \tag{2g}$$

where

$$C_u = \frac{AP}{2-(j+1)K}\frac{C_\alpha}{\alpha_0}, \tag{2h}$$

$$C_\rho = -\rho_0 P \frac{C_\alpha}{\alpha_0}, \tag{2i}$$

$$P = \frac{\alpha_0}{1+\alpha_0} - \frac{\alpha_0}{4+\alpha_0}\left(1+\frac{\theta}{T_0}\right), \tag{2j}$$

and A, α_0, ρ_0, T_0, C_α are constants obtained numerically for specific examples. Equations (2) describe the inviscid flow near the wall, and we will use them to deduce the behaviour of the boundary layer.

The inner expansion

The inner region lies near the wall, and its scale is of the order of the viscous length. We expand the variables in powers of x, as in the outer region, and then magnify the normal velocity component and co-ordinate by the square root of the Reynolds number, as dictated by boundary-layer theory. The leading term of the inner expansion will then describe the conventional stagnation-point boundary layer. Our point of view is that unless otherwise proved wrong, this should be expected to be the first approximation to the flow. The secondary term is of an order ϵ, to be determined by matching to the outer flow. The resulting inner expansion is of the form

$$\alpha(x, \eta; R) = \alpha_{i1}(\eta) + \epsilon(R)\,\alpha_{i2}(\eta) + \ldots + O(x^2), \quad \epsilon \to 0. \tag{3}$$

Further details are presented in the appendix, in equations (A 5). Substitution of the inner expansions into the Navier–Stokes equations (A 1) yields the first-order inner equations (A 6) and the second-order inner equations (A 7). Similar substitutions give the corresponding boundary conditions.

The first-order inner problem

This problem is governed by equations (A 6) and the boundary conditions listed below them. It is the conventional problem for the stagnation-point boundary layer, and need not be reviewed here in its details. Matching to the first-order outer solution confirms that this is the appropriate first approximation to the flow, the outer singularity notwithstanding. This is so because the outer singularity affects only the derivatives of the outer solution, and these do not enter into the matching process to the present order. The outer functions themselves have finite values at the wall (equations (2)), and the inner functions approach these values asymptotically. It is true that each of the outer functions reaches its asymptote with infinite first derivative whereas the inner do so with vanishing derivative, but this apparent discrepancy is irrelevant to the present order, and will be accounted for in the higher approximations. Numerical results for the inner problem are discussed in § 3.

The second-order inner problem

In this problem the effects of the outer singularity are felt in full force, because the far boundary conditions (as $\eta \to \infty$) and the form of the parametric function ϵ in the inner expansion are imposed by the outer solution. To illustrate this interaction we follow the matching process in detail for our sample variable α. In order to involve the second-order inner functions, the matching must be carried out at least to order $R^{-\frac{1}{2}K}$. The outer expansion (1), to relative order $R^{-\frac{1}{2}K}$, is

$$\alpha = \alpha_1(y). \tag{4a}$$

In inner variables,
$$\alpha = \alpha_1[\eta/(AR)^{\frac{1}{2}}]. \tag{4b}$$

Expanded to relative order $R^{-\frac{1}{2}K}$, $(R \to \infty)$, with the use of (2e), this gives

$$\alpha = \alpha_0 + C_\alpha[\eta^K/(AR)^{\frac{1}{2}K}]. \tag{4c}$$

This indicates that in the inner expansion (3), $\epsilon(R)$ must be of order $R^{-\frac{1}{2}K}$, since then the inner expansion to that order is

$$\alpha = \alpha_{i1}(\eta) + \epsilon(R)\,\alpha_{i2}(\eta), \tag{4d}$$

and in outer variables

$$\alpha = \alpha_{i1}[(AR)^{\frac{1}{2}}y] + \epsilon\alpha_{i2}[(AR)^{\frac{1}{2}}y]. \tag{4e}$$

Expanded to relative order $R^{-\frac{1}{2}K}$, $(R \to \infty)$, this gives

$$\alpha = \alpha_{i1}(\eta) + \epsilon\alpha_{i2}(\eta), \quad \eta \to \infty. \tag{4f}$$

Following the matching rule, we equate (4f) and (4c). We already noted that the first-order function approaches the inviscid value at the wall; that is, $\alpha_{i1}(\infty) = \alpha_0$. The second-order matching condition is then

$$\epsilon\alpha_{i2} \to C_\alpha[\eta^K/(AR)^{\frac{1}{2}K}] \quad \text{as} \quad \eta \to \infty.$$

For convenience we absorb the factor $A^{\frac{1}{2}K}$ into ϵ, and set

$$\epsilon = 1/(AR)^{\frac{1}{2}K}, \quad \alpha_{i2} \to C_\alpha \eta^K \quad \text{as} \quad \eta \to \infty. \tag{5}$$

The rest of the variables are matched in a similar way, and the results are given in the appendix. Equations (5) summarize the novel features of the present problem. The second-order boundary layer is of order $R^{-\frac{1}{2}K}$ instead of the conventional $R^{-\frac{1}{2}}$, and the functions of η are new, since far from the wall each behaves like a non-integral power of the distance instead of approaching a constant or an integral power as in the conventional second-order boundary layer. The fact that the reaction parameter K appears in the exponent of the Reynolds number is of significance, because in slowly reacting flows of practical importance K may be as small as one-tenth or one-hundredth. In such cases, $R^{-\frac{1}{2}K}$ will be a much larger number than $R^{-\frac{1}{2}}$, as the reader may be surprised to discover with a quick calculation. However, the threat of an exceptionally large second-order correction does not seem to materialize in the present case. A few numerical examples

(§ 3) show that as $K \to 0$ the increase in ϵ is offset by a decrease in α_{i2}. Nevertheless, this compensating effect may not be universal, and one should be warned of the possibility of large corrections due to the outer singularity.

In order to study the structure of the solutions far from the wall, we investigate the second-order differential equations (A 7) as $\eta \to \infty$. The coefficients of these equations contain the first-order variables, and we assign to them their asymptotic values $\alpha_0, \rho_0, h_0, T_0$, 1 (for u_{i1}) and $\eta - \beta$ (for v_{i1}), where β is the displacement thickness. These variables approach their asymptotes exponentially, with an error of order $\exp(-\eta^2)$. We look for solutions of the asymptotic differential equations in the form of power series, the leading term being of the required type $C\eta^K$. Substitution into the differential equations shows that such solutions exist, and are:

$$\frac{\alpha_{i2}}{C_\alpha} = \frac{u_{i2}}{C_u/A} = \frac{\rho_{i2}}{C_\rho} = \eta^K\left[1 - \beta K\eta^{-1} - \left(\frac{1}{\rho_0} + \beta^2\right)\frac{K(1-K)}{2}\eta^{-2} + O(\eta^{-3})\right], \quad (6a)$$

$$v_{i2} = \frac{1}{1+K}\left(\frac{Cu}{A} + PKC_\alpha\right)\eta^{1+K}[1 - (1+K)\beta\eta^{-1} + O(\eta^{-2})]. \quad (6b)$$

The variables h_{i2} and p_{i2}, which do not match singular terms in the outer expansion, approach zero to any algebraic order as $\eta \to \infty$. Equations (6) show the algebraic structure of the second-order functions in the outer fringes of the boundary layer. This structure differs from the conventional exponential decay, but it should not be construed as an algebraic decay in an absolute sense, since the outer flow matches this behaviour at least to second order, and probably to higher orders as well. We shall return to this matter and elaborate on the decay of vorticity in a later section. The numerical solution of the second-order problem is discussed in § 3.

Higher orders in the inner expansion

The sample matching of the previous section reveals several features of the inner expansion. It is clear that as the matching process is carried out to higher orders, more terms of (2d) will enter in (4c), and will have to be matched by (4d). That is, the inner expansion will include terms of order $R^{-\frac{1}{2}K}, R^{-K}, R^{-\frac{1}{2}(1+K)}, \ldots$, all of which match the first-order outer solution. The situation differs from the conventional one, where matching proceeds term by term, alternating between the outer and inner expansions. We see then that the inviscid singularity has spawned a number of new higher-order boundary layers, and this number grows without bound as $K \to 0$.

It is of interest to see how the conventional second-order boundary layer is recovered. The transition occurs at $K = 1$, which is a singular case as explained by Conti & Van Dyke (1969). Without dwelling on this case, we note that when $K > 1$, matching to order $R^{-\frac{1}{2}K}$ requires that the outer expansion (1) be considered at least to the second order, $R^{-\frac{1}{2}}$. Thus, (4a) becomes

$$\alpha = \alpha_1(y) + \frac{1}{R^{\frac{1}{2}}}\alpha_2(y) + \ldots,$$

and (4c) becomes
$$\alpha = \alpha_0 + \frac{1}{R^{\frac{1}{2}}}\alpha_2(0) + \ldots + \frac{1}{R^{\frac{1}{2}K}}\frac{C_\alpha \eta^K}{A^{\frac{1}{2}K}}.$$

Now the secondary term is given by the conventional flow due to displacement thickness, and the matching boundary layer will be the conventional second-order one. This completes the ranking of the new terms in the inner expansion. In slowly reacting flows ($0 < K < 1$) one or more of the new terms, derived from the inviscid singularity, are the leading corrections to the classical first-order boundary layer. In rapidly reacting flows ($1 < K \leqslant \infty$) the leading correction is given by the usual second-order boundary layer, and the new terms are of some higher order.

Decay of vorticity

We noted earlier that in slowly reacting flows the singularity in the inviscid flow creates a new form of higher-order boundary layer, having an algebraic structure far from the wall. In particular, this involves an algebraic decrease of vorticity. Since in ordinary forced-convection flows there are compelling physical reasons for the vorticity in the boundary layer to decay exponentially to the outer value, the algebraic behaviour of the new boundary layer should be regarded with suspicion. To scrutinize this matter we use the inner expansions (A 5) to compute the magnitude of the vorticity in the boundary layer, and find that

$$\Omega = \frac{\partial u}{\partial y} - \frac{\partial v}{\partial x} = \frac{A^{\frac{3}{2}}}{j+1} R^{\frac{1}{2}} x[u'_{i1}(\eta) + \epsilon u'_{i2}(\eta) + \ldots] + O(R^{-\frac{1}{2}}).$$

As $\eta \to \infty$ the function u'_{i1} (from classical boundary-layer theory) is of order $\exp(-\eta^2)$. Any contributions to algebraic decay must come from u'_{i2} and the successive higher-order terms. From (6*a*), as $\eta \to \infty$

$$u'_{i2} = K\frac{C_u}{A}\eta^{K-1}\left[1 - \beta(K-1)\eta^{-1} - \left(\frac{1}{\rho_0} + \beta^2\right)\frac{(1-K)(K-2)}{2}\eta^{-2} + O(\eta^{-3})\right]. \tag{7}$$

Here the first term is the asymptotic value of u'_{i2} that matches the first-order outer flow, and the rest of the terms describe the decaying function. On first inspection it seems that the decay is algebraic, but this is true only when it is measured from the first-order level. Instead, the decay should be measured from the actual level in the outer flow. Should higher approximations in the outer flow contain terms that match every term in (7) and in the higher orders, the algebraic contributions to the decay of vorticity would vanish. To furnish such proof is out of the present scope, but it seems natural to search for the would-be partner of the first 'decay' term, that involving $\beta(1-K)\eta^{-1}$ in (7). In outer variables this is $\beta(1-K)/[y(AR)^{\frac{1}{2}}]$ and therefore the outer partner belongs in the flow due to displacement thickness, represented by $\alpha_2(y)$ in (1). To establish (or rule out) the actual existence of such a term in the outer flow, we need the asymptotic solution of the second-order outer problem as $y \to 0$. We obtain this solution by substitution of power series into the outer equations (A 4), but we will omit a detailed account. The results show that the flow due to displacement thickness indeed matches our term $\beta(1-K)\eta^{-1}$ and all corresponding terms for the other variables. This, of course, does not prove that the vorticity decays exponentially, but it shifts the burden of proof. From the regular ordering of the problem it seems likely that the process will be repeated in higher orders, and the exponential decay of the first-order term will prevail.

Composite solution

After obtaining outer and inner solutions we wish to combine them, without loss of accuracy, into a composite that is valid in both regions. Such a composite is not unique, and there are several ways of forming it. We adopt the additive rule; that is, we add the outer and inner solutions and subtract the inner expansion of the outer expansion to get, for the sample variable α:

$$\alpha_c = \alpha_{\text{outer}} + \alpha_{\text{inner}} - [\alpha_0 + C_\alpha \eta^K/(AR)^{\frac{1}{2}K}].$$

This result has a disturbing feature that derives from the singularity in the outer solution. This can be examined by expanding the composite near the wall. For the outer function we use ($2d$) rewritten in inner variables, and obtain

$$\begin{aligned}\alpha_c &= \alpha_0 + C_\alpha \eta^K/(AR)^{\frac{1}{2}K} + O[\eta^{2K}/(AR)^K] + \alpha_{i1} + \alpha_{i2}/(AR)^{\frac{1}{2}K} - [\alpha_0 + C_\alpha \eta^K/(AR)^{\frac{1}{2}K}],\\ &= \alpha_{i1} + \alpha_{i2}/(AR)^{\frac{1}{2}K} + O[\eta^{2K}/(AR)^K].\end{aligned}$$

This recovers the inner solution, with higher-order terms left over from the outer. It is precisely in these higher-order terms that the difficulty lies, because they are singular at the wall. For example, for $K < \frac{1}{2}$ the first derivative of the composite is infinite at $\eta = 0$. This situation worsens as $K \to 0$. We see by inspection that if the outer singularity involves a finite number of terms, an equal number of higher-order approximations in the boundary layer will remove the difficulty. Short of this goal, as more higher-order approximations are calculated, the anomaly is shifted to a higher derivative. The composite solution can still be used to link inner and outer flows, but its usefulness to calculate derivatives at the wall is limited. The numerical results of § 3 illustrate this problem.

3. Numerical results

The first-order outer problem and the first-order and second-order inner problems are solved numerically with the help of a high-speed computer. These problems involve ordinary differential equations, which are integrated using a standard Runge–Kutta technique. We discuss an example of axisymmetric flow over a body having a catalytic wall, with the data shown in table 1. The free-stream conditions are typical of a sub-orbital ballistic re-entry into the atmosphere. The parameters in the ideal dissociating gas correspond to oxygen and nitrogen, mass-averaged according to their proportions in the atmosphere. The rate of reaction appears in the parameter Γ, which is taken as constant in the ideal dissociating model. Calculations using a more realistic model of a diatomic gas show that Γ varies substantially across the shock layer, and one should be prepared to accept a factor of 10 as a typical uncertainty. Accordingly, we consider three examples where all other parameters remain the same, but Γ ranges over an order of magnitude. This serves the further purpose of studying the effect of a change in the reaction parameter K at fixed Reynolds number.

The outer problem is discussed in detail by Conti & Van Dyke (1969). The integration proceeds from the shock wave to the body. The singularity at the stagnation point is of the stable-equilibrium type, and it fixes the values of A, C_α, and, say, p_0. These quantities are sufficient to determine all other characteristics of the stagnation point, such as the state of the gas and the reaction parameter K. Selected results are shown in table 1.

Free stream	Ideal dissociating gas	Shock wave	Body
Speed: 5·9972 km/sec	Dissociation temperature: 102,300 °K	Radius: 5 cm	Axisymmetric. Catalytic wall.
Density: $3{\cdot}48\times10^{-6}$ g/cm^3 (altitude 41 km)	Dissociation density: 134 g/cm^3	Density ratio: 1/7	Wall temperature: 2000 °K
	Molecular gas constant: 287 m^2/(°K sec^2)		

Dimensionless variables

$(\theta = 40, \quad \rho_d = 5{\cdot}5\times10^6, \quad h_0 = 2{\cdot}45, \quad R = 10{,}443.)$

Γ	K	C_α	A	p_0	α_0	ρ_0	Δ	β
$3{\cdot}900\times10^4$	0·0498	−0·0285	5·4630	6·6226	0·3488	2·0244	0·0636	0·3824
$1{\cdot}422\times10^5$	0·1843	−0·0475	5·4312	6·6601	0·3487	2·0354	0·0580	0·3821
$3{\cdot}900\times10^5$	0·5110	−0·1651	5·4102	6·6862	0·3486	2·0430	0·0542	0·3831

TABLE 1. Free-stream conditions and selected results.

The first-order inner problem describes the conventional stagnation-point boundary layer. The points $\eta = 0$ and $\eta = \infty$ are critical points of the system. Marching integration, either forward (increasing η) or backward (decreasing η), involves the guessing of three constants at the initial point, and iterations thereof until all boundary conditions at the opposite end are satisfied. Forward integration is unstable (and backward is stable), but due to the simplicity of the present problem a practical way was found to deal with the instability of the conventional forward integration. This is based on the observation that if we follow the spurious solutions (rather than abandoning them soon after they depart from the correct behaviour) they eventually fall into the form

$$u_{i1} = A_1+A_2\eta, \quad h_{i1} = A_3, \quad \rho_{i1} = A_4,$$

where the A_i are constants. At this point we can stop the integration and iterate on the initial unknowns so as to make $A_2 \to 0$, $A_3 \to h_0$, $A_4 \to \rho_0$. This will make $A_1 \to 1$, and the solution will approach the correct one. The iteration process is stopped, and the solution accepted, when the variables attain their correct asymptotic value within 10^{-6}, with derivatives smaller than 10^{-8}, at $\eta = 5$.

The second-order inner problem is linear. We exploit this fact by constructing the solution through a linear combination of any three solutions, obtained by assigning arbitrary values (say, 1 and 0) to the unknown quantities at $\eta = 0$. The linear combination is then formulated in such a way that equations (6) are satisfied at a large η, say $\eta = 50$. To test the accuracy of the results a new integration is

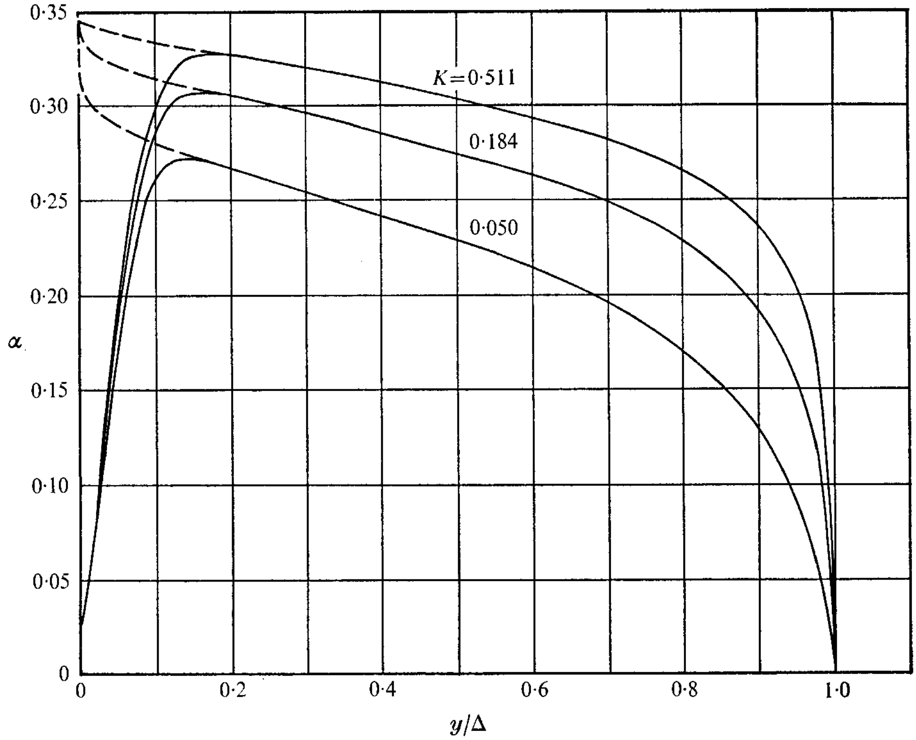

FIGURE 2. Degree of dissociation in the shock layer. The outer variable y is referred to the standoff distance. The composite solution is shown in solid lines, the outer solution in broken lines.

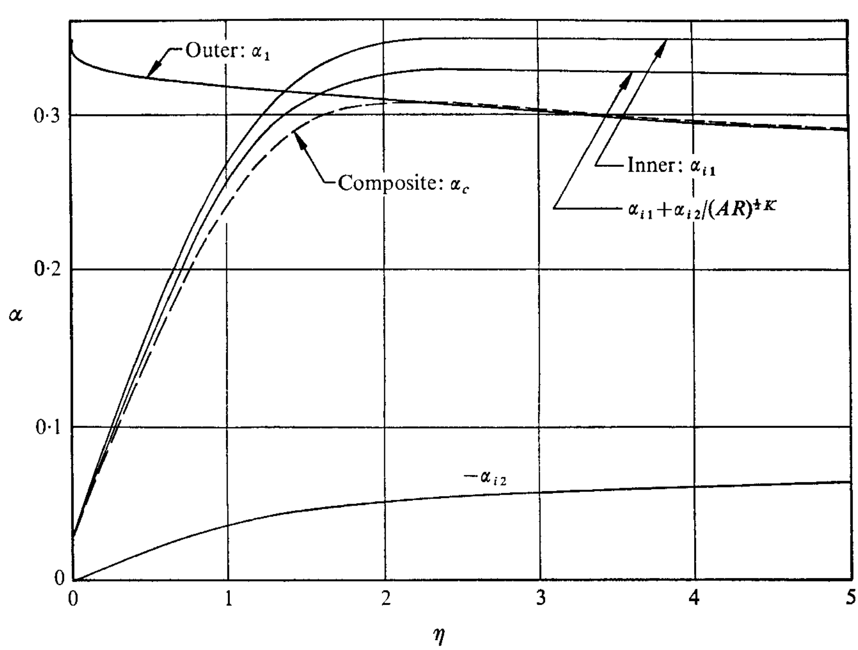

FIGURE 3. Degree of dissociation in the boundary layer for $K = 0{\cdot}184$.

performed using the initial conditions obtained in the previous step, and the results tested against equations (6) at regular intervals, up to $\eta = 100$. A solution is accepted when the variables differ from equations (6) by less than 10^{-3}.

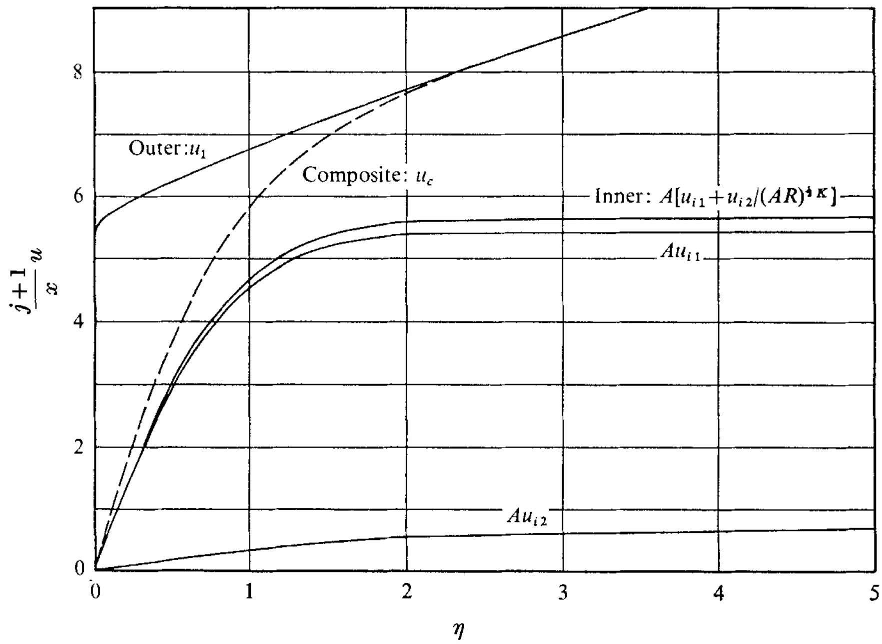

FIGURE 4. Tangential velocity component in the boundary layer for $K = 0{\cdot}184$.

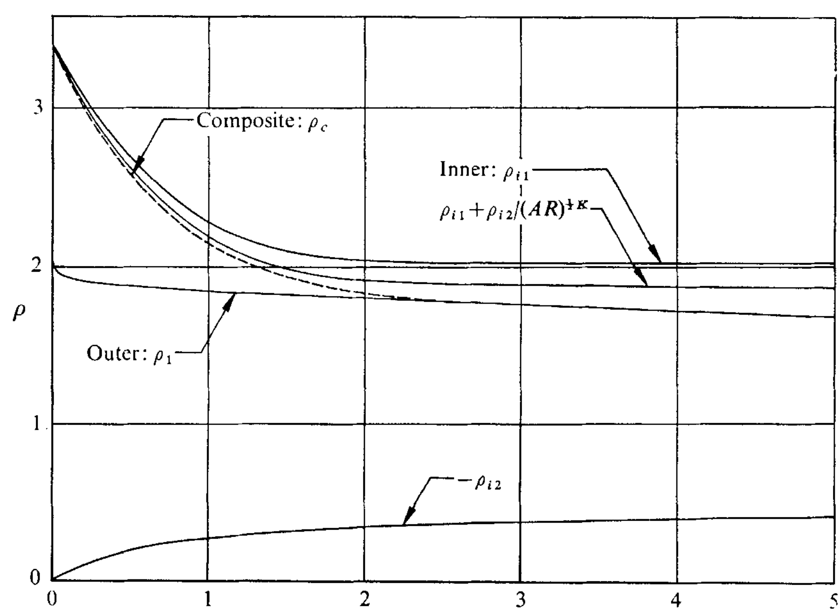

FIGURE 5. Density in the boundary layer for $K = 0{\cdot}184$.

Some numerical results, obtained under the conditions listed in table 1, are shown in figures 2–9. Figure 2 gives an over-all view of the degree of dissociation in the shock layer, for several values of K. In particular we note the singular behaviour of the outer solution near the wall (broken lines), and how this is

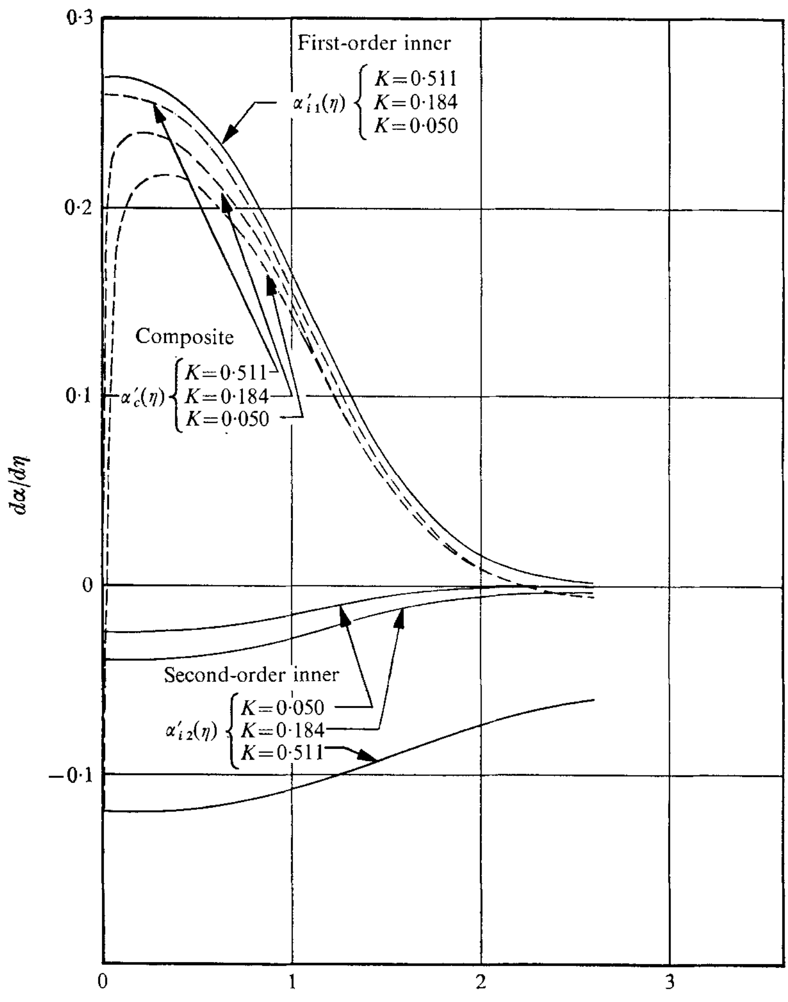

FIGURE 6. First derivative of the degree of dissociation in the boundary layer, showing the singularity in the composite solution.

modified by the boundary layer. Figures 3–5 show the variables in the boundary layer for $K = 0{\cdot}184$. The inner solution is shown to first and second orders, and the outer solution (in terms of the inner variable η) is included for comparison. We note how the composite solution merges with the inner and the outer solutions. The anomalous behaviour of the composite solution near the wall, which we discussed earlier, is not visible to the scale of the drawings. To illustrate the problem we refer to figure 6, showing the first derivative of the degree of dissociation. As we recall, the troublesome term in the composite solution is of order

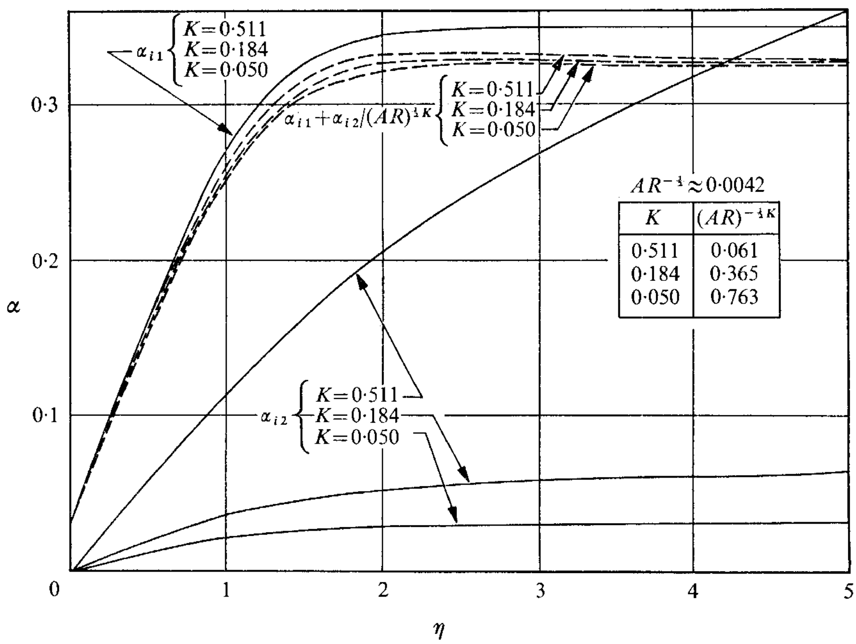

FIGURE 7. Effect of the reaction parameter K on the degree of dissociation, illustrating the lack of sensitivity of the second-order correction.

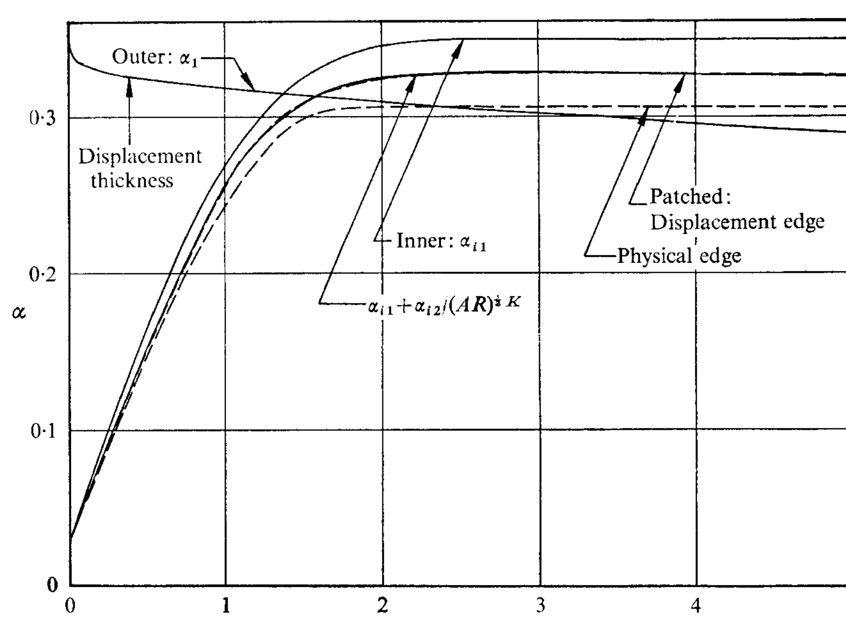

FIGURE 8. Effect of patching the first-order boundary layer to the displacement and physical edges.

η^{2K} near the wall. The first derivative, of order η^{2K-1}, is infinite for $K < \frac{1}{2}$ but finite otherwise. Figure 6 shows the singularity for $K = 0{\cdot}050$ and $K = 0{\cdot}184$, and its absence at $K = 0{\cdot}511$. Again, the singularity in the next higher derivative, which affects all cases shown, is lost to the eye at $K = 0{\cdot}511$ in the present scale of the drawing.

Figure 7 illustrates the effect of the reaction parameter K on the magnitude of the second-order correction. As $K \to 0$ the second-order factor $(AR)^{-\frac{1}{2}K}$ increases drastically as indicated in the insert, but at the same time the function α_{i2} decreases in such a way that the overall correction (in broken lines) remains roughly the same.

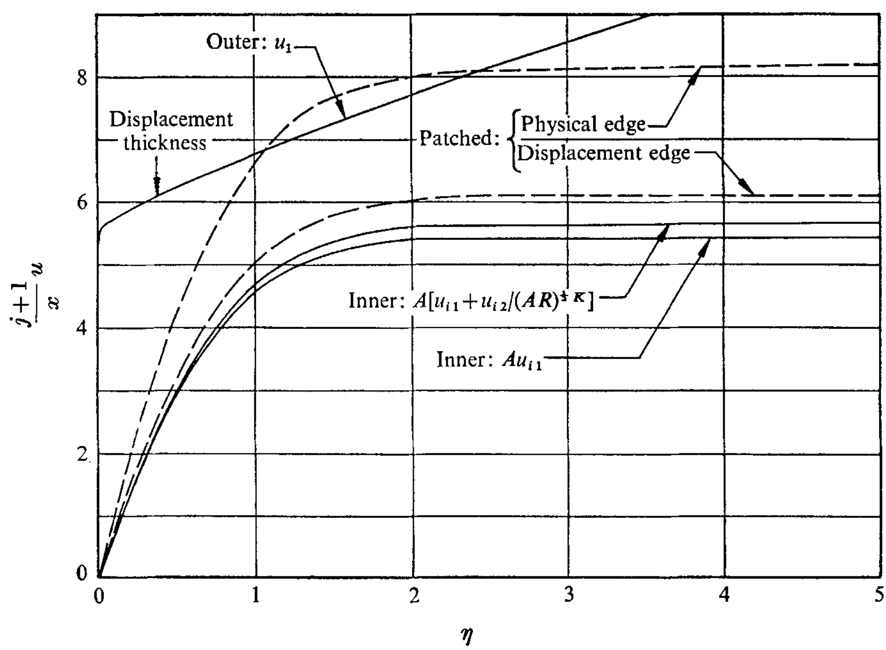

FIGURE 9. Effect of patching the first-order boundary layer to the displacement and physical edges.

The difference between systematic boundary-layer theory and 'patching' is shown in figures 8 and 9. Here the boundary-layer results are presented to first and second order. The patching consists in calculating the first-order boundary layer with the boundary conditions at $\eta = \infty$ corresponding to some point in the interior of the inviscid flow. Two sets of patched solutions are presented, with the interior point located either at the displacement thickness or at the 'physical thickness' (where the velocity differs by $0{\cdot}1\,\%$ from the asymptotic value at infinity). Patching at the displacement thickness yields a degree of dissociation that agrees very well with the boundary-layer result to second order, but this must be regarded as largely fortuitous. The tangential velocity does not agree equally well. Furthermore, the results are sensitive to the selection of the point of patching. On the other hand, we note that in general the results of patching differ from the correct first-order boundary layer in the proper direction, as estimated from the second-order correction. A further assessment of the errors involved in patching can be obtained by comparing the first derivatives of flow variables at the wall, which are presented in table 2.

		Derivative $(d/dy)_{y=0}$			
Variable	K	First order	First plus second order	Patched (displacement thickness)	Patched (physical thickness)
$[(j+1/x)]\,u$	0·511	1714·8	1746·4	1854·7	2462·0
	0·184	1721·4	1753·5	1863·6	2413·6
	0·050	1731·8	1766·7	1867·8	2335·9
α	0·511	63·575	61·907	62·708	60·701
	0·184	63·919	60·447	59·821	56·515
	0·050	64·088	59·487	54·331	49·260
ρ	0·511	−435·47	−405·46	−441·41	−455·66
	0·184	−429·01	−480·29	−465·58	−494·30
	0·050	−424·22	−489·34	−528·15	−565·87
h	0·511	3157·6	3166·5	3140·8	3103·9
	0·184	3159·0	3153·1	3098·9	3048·9
	0·050	3159·7	3146·4	3020·7	2965·4

TABLE 2. Derivatives at the wall, from the inner solution.

4. Concluding remarks

The previous results establish the general structure that the boundary layer will assume in the presence of an external singularity of algebraic type. To display this structure we write the outer solution near the wall and the inner solution far away from it, with matching terms arranged in columns. Selecting the range $\frac{1}{3} < K < \frac{1}{2}$ as an example, we write the following for the tangential velocity,

Outer:

$$\frac{j+1}{x}u = A + C_u y^K + D_u y^{2K} + E_u y^2 + \dots + \frac{1}{R^{\frac{1}{2}}}\left[-\frac{\beta K C_u}{A^{\frac{1}{2}}} y^{K-1} + O(y^{2K-1}) + O(\beta) + \dots\right] + O\left(\frac{1}{R}\right)$$

Inner:

$$\begin{array}{llllll}
= A + \exp & & & & & \\
+\dfrac{1}{(AR)^{\frac{1}{2}K}}\,[\;C_u\eta^K & & -\beta K C_u \eta^{K+1} & & & +O(\eta^{K-2})] \\
+\dfrac{1}{(AR)^{K}}\,[& O(\eta^{2K}) & & +O(\eta^{2K-1}) & & +O(\eta^{2K-2})] \\
+\dfrac{1}{(AR)^{\frac{1}{2}}}\,[& & & & +O(\beta) & +\exp] \\
+\dots & & & & &
\end{array}$$

In the outer expansion the conventional terms are the ones in integral powers (a linear term in y would be added if we had external vorticity, and this would be matched by a term of order η in the last row of the inner expansion). The inner expansion is led by Prandtl's boundary layer (first row), which is followed by two new corrections, forced by the non-integral powers in the outer expansion. The conventional second-order boundary layer (last row) enters through the displacement effect (of order β), and becomes the leading correction as soon as K exceeds unity. The previous expansions show the general ranking of terms within each approximation, and the ordered pairing of the new, non-integral powers.

The authors are indebted to P. D. Thomas for advice on the integration of differential equations with singular end-points, and to H. Kirch for programming and executing the numerical integration.

Appendix

Dimensionless variables and governing equations

We consider the flow of an ideal dissociating gas (Lighthill 1957) in the vicinity of a blunt stagnation point. The flow variables are made dimensionless by reference to the radius of curvature of the shock wave r_s and the normal velocity and density behind the shock wave, v_s and ρ_s. Thus, the co-ordinates x and y are referred to r_s, the velocity components u and v to v_s, the density ρ to ρ_s, the pressure p to $\rho_s v_s^2$, the enthalpy h to v_s^2, and the temperature T to v_s^2/R_m, where R_m is the molecular gas constant. The dimensionless degree of dissociation (atom mass-fraction) is denoted by α, and its fictitious 'local equilibrium' value by α^*. The parameters appearing in the equations are the Reynolds number $R = (\rho_s v_s r_s)/\mu$, the characteristic density of dissociation ρ_d (referred to ρ_s), the characteristic temperature of dissociation θ (referred to v_s^2/R_m), the rate of reaction Γ (referred to $v_s/(r_s\rho_s)$), and the constant j, equal to one for axisymmetric flow and zero for planar flow. The Prandtl and Lewis numbers are assumed to be unity, and the coefficient of viscosity μ to be constant. With the previous definitions and assumptions the conservation equations (Navier–Stokes) are as follows:

Mass:

$$\frac{\partial}{\partial x}(x^j\rho u)+\frac{\partial}{\partial y}(x^j\rho v) = 0. \tag{A 1a}$$

x-Momentum:

$$\rho u\frac{\partial u}{\partial x}+\rho v\frac{\partial u}{\partial y} = -\frac{\partial p}{\partial x}+\frac{1}{R}\left[\frac{4}{3}\frac{j}{x}\left(\frac{\partial u}{\partial x}-\frac{u}{x}\right)+\frac{4}{3}\frac{\partial^2 u}{\partial x^2}+\frac{1}{3}\frac{\partial^2 v}{\partial y\,\partial x}+\frac{\partial^2 u}{\partial y^2}\right]. \tag{A 1b}$$

y-Momentum:

$$\rho u\frac{\partial v}{\partial x}+\rho v\frac{\partial v}{\partial y} = -\frac{\partial p}{\partial y}+\frac{1}{R}\left[\frac{j}{x}\left(\frac{1}{3}\frac{\partial u}{\partial y}+\frac{\partial v}{\partial y}\right)+\frac{1}{3}\frac{\partial^2 u}{\partial x\,\partial y}+\frac{\partial^2 v}{\partial x^2}+\frac{4}{3}\frac{\partial^2 v}{\partial y^2}\right]. \tag{A 1c}$$

Energy:

$$\rho u\frac{\partial h}{\partial x}+\rho v\frac{\partial h}{\partial y} = u\frac{\partial p}{\partial x}+v\frac{\partial p}{\partial y}+\frac{1}{R}\left[-\frac{2}{3}\left(j\frac{u}{x}+\frac{\partial u}{\partial x}+\frac{\partial v}{\partial y}\right)^2+j\left(\frac{u}{x}\right)^2+\left(\frac{\partial v}{\partial x}\right)^2\right.$$
$$\left.+\left(\frac{\partial v}{\partial y}\right)^2+\frac{1}{2}\left(\frac{\partial u}{\partial y}+\frac{\partial v}{\partial x}\right)^2+\frac{j}{x}\frac{\partial h}{\partial x}+\frac{\partial^2 h}{\partial x^2}+\frac{\partial^2 h}{\partial y^2}\right]. \tag{A 1d}$$

Species:

$$\rho u\frac{\partial\alpha}{\partial x}+\rho v\frac{\partial\alpha}{\partial y}=\frac{\Gamma}{\rho_d}\rho^3\left(\frac{\alpha^*}{1-\alpha^*}+\alpha\right)(\alpha^*-\alpha)+\frac{1}{R}\left(\frac{j}{x}\frac{\partial\alpha}{\partial x}+\frac{\partial^2\alpha}{\partial x^2}+\frac{\partial^2\alpha}{\partial y^2}\right). \quad (\mathrm{A}\,1e)$$

State: $$p=(1+\alpha)\rho T,\quad h=(4+\alpha)T+\theta\alpha. \quad (\mathrm{A}\,1f,g)$$

Law of mass action: $$\frac{\alpha^{*2}}{1-\alpha^*}=\frac{\rho_d}{\rho}\exp\left(-\frac{\theta}{T}\right). \quad (\mathrm{A}\,1h)$$

Boundary conditions

On the downstream face of the shock wave the translational and rotational degrees of freedom of the molecules are assumed in equilibrium, and molecular vibration is assumed half-excited, as required by the ideal dissociating gas. The degree of dissociation is assumed to be zero. Under these conditions the ideal dissociating gas has a ratio of specific heats $\gamma=\frac{4}{3}$. For hypersonic flight conditions with negligible upstream pressure, the density ratio across the shock wave is then $\kappa\approx(\gamma-1)/(\gamma+1)=\frac{1}{7}$, and the boundary conditions for the flow variables near the dividing streamline are: $u=x/\kappa$, $v=-1$, $\rho=1$, $\alpha=0$, $p=T=\frac{1}{4}h=(1-\kappa)/\kappa$ and $\alpha^*=0{\cdot}999857$ (from (A 1h)). On the body the boundary conditions are $u=v=0$, $T=T_w=$ constant, and $\alpha=\alpha^*$ (catalytic wall), or $d\alpha/dy=0$ (inert wall).

Outer flow

In the outer ('inviscid') region the independent variables are x and y (figure 1) and the dependent variables are expanded as follows (with $\delta=1/R^{\frac{1}{2}}$):

$$\frac{j+1}{x}u(x,y;R)=u_1(y)+\delta u_2(y)+\ldots+O(x^2), \quad (\mathrm{A}\,2a)$$

$$-v(x,y;R)=v_1(y)+\delta v_2(y)+\ldots+O(x^2), \quad (\mathrm{A}\,2b)$$

$$p(x,y;R)=p_1(y)+\delta p_2(y)+\ldots+x^2[p_{12}(y)+\delta p_{22}(y)]+O(x^4). \quad (\mathrm{A}\,2c)$$

All other thermodynamic variables follow the form of p.

First-order outer equations. The arrangement of the equations is the same as in (A 1)

$$\rho_1u_1-(\rho_1v_1)'=0, \quad (\mathrm{A}\,3a)$$

$$\rho_1v_1u_1'-\rho_1u_1^2/(j+1)-2(j+1)p_{12}=0, \quad (\mathrm{A}\,3b)$$

$$\rho_1v_1v_1'+p_1'=0, \quad (\mathrm{A}\,3c)$$

$$h_1+v_1^2/2=h_0=\text{constant}, \quad (\mathrm{A}\,3d)$$

$$v_1\alpha_1'+\frac{\Gamma}{\rho_d}\rho_1^2\left(\frac{\alpha_1^*}{1-\alpha_1^*}+\alpha_1\right)(\alpha_1^*-\alpha_1)=0, \quad (\mathrm{A}\,3e)$$

$$p_1=(1+\alpha_1)\rho_1T_1, \quad (\mathrm{A}\,3f)$$

$$h_1=(4+\alpha_1)T_1+\theta\alpha_1, \quad (\mathrm{A}\,3g)$$

$$\frac{\alpha_1^{*2}}{1-\alpha_1^*}=\frac{\rho_d}{\rho_1}\exp\left(-\frac{\theta}{T_1}\right). \quad (\mathrm{A}\,3h)$$

Assumption: $p_{12}=[-p_1/(r_b+y)^2]+\{p_1'/[2(r_b+y)]\}$, where r_b is the dimensionless distance between the stagnation point and the centre of curvature of the shock wave. This assumption is a variation of the method of series truncation, and the form of p_{12} is dictated by the choice of co-ordinate system (see the last section of the appendix).

First-order outer boundary conditions. At the shock wave $u_1 = (j+1)/\kappa$, $v_1 = \rho_1 = 1$, $\alpha_1 = 0$ and $p_1 = (1-\kappa)/\kappa$. The body is located at the point where $v_1 = 0$.

The first-order outer problem is non-linear, and can be solved as an initial-value problem (inverse method for flow behind a given shock wave). The differential equations have a node-like singularity at the body that sets the values of the inviscid stagnation-point quantities p_0, α_0, ρ_0, etc., as well as the constants A, C_α, C_u, K, etc., discussed in the text. Further details about this problem, including the series-truncation assumption, are discussed in Conti & Van Dyke (1969).

Second-order outer equations

$$\rho_1 u_2 + u_1 \rho_2 - (v_1 \rho_2 + \rho_1 v_2)' = 0, \tag{A 4a}$$

$$\rho_1 v_1 u_2' - \frac{2}{j+1}\rho_1 u_1 u_2 + \rho_1 u_1' v_2 + \left(v_1 u_1' - \frac{u_1^2}{j+1}\right)\rho_2 - 2(j+1)\,p_{22} = 0, \tag{A 4b}$$

$$\rho_1 v_1 v_2' + \rho_1 v_1' v_2 + v_1 v_1' \rho_2 + p_2' = 0, \tag{A 4c}$$

$$\rho_1 v_1 h_2' + v_1 h_1' \rho_2 - v_1 p_2' = 0, \tag{A 4d}$$

$$\frac{\alpha_2'}{\alpha_1'} + \frac{v_2}{v_1} + 4\frac{\rho_2}{\rho_1} + \frac{\alpha_2^* - \alpha_2}{\alpha_1^* - \alpha_1} + \frac{\alpha_2^* + (1-\alpha_1^*)^2 \alpha_2}{(1-\alpha_1^*)\,\alpha_1^* + (1-\alpha_1^*)^2 \alpha_1} = 0, \tag{A 4e}$$

$$\frac{p_2}{p_1} = \frac{\alpha_2}{1+\alpha_1} + \frac{T_2}{T_1} + \frac{\rho_2}{\rho_1}, \tag{A 4f}$$

$$h_2 = (T_1 + \theta)\,\alpha_2 + (4+\alpha_1)\,T_2, \tag{A 4g}$$

$$\alpha_2^* = \frac{\alpha_1^*(1-\alpha_1^*)}{2-\alpha_1^*}\left(\frac{\theta}{T_1}\frac{T_2}{T_1} - \frac{\rho_2}{\rho_1}\right), \tag{A 4h}$$

Second-order outer boundary conditions. At the shock wave

$$u_2 = v_2 = \rho_2 = p_2 = \alpha_2 = 0.$$

Unknown: v_2'. At the body the normal velocity v_2 is the 'displacement velocity' from the first-order boundary layer, and is determined by matching to the first-order inner solution.

The second-order outer problem (examined only asymptotically in the present work) is linear and can be solved by superposition of arbitrary solutions to satisfy the shock and displacement-velocity conditions.

Inner flow

The inner (boundary-layer) region has a thickness of order $\delta = 1/R^{\frac{1}{2}}$. The independent variables are $x = x$ and $\eta = A^{\frac{1}{2}}y/\delta$, where $A = u_1(0)$ is a constant proportional to the velocity gradient at the stagnation point in the outer flow. In the inner region the dependent variables (denoted by the subscript i) are expanded as follows:

$$\frac{j+1}{x}\,u(x,\eta;\,R) = A[u_{i1}(\eta) + \epsilon u_{i2}(\eta) + \ldots + O(x^2)], \tag{A 5a}$$

$$-v(x,\eta;\,R) = A^{\frac{1}{2}}\delta[v_{i1}(\eta) + \epsilon v_{i2}(\eta) + \ldots + O(x^2)], \tag{A 5b}$$

$$p(x,\eta;\,R) = p_{i1}(\eta) + \epsilon p_{i2}(\eta) + \ldots + x^2[p_{i12}(\eta) + \epsilon p_{i22}(\eta) + \ldots] + O(x^4), \tag{A 5c}$$

with all other thermodynamic variables having the same form as p. The small parameter $\epsilon(R)$ is determined by matching to the outer solution and is $\epsilon = \delta^K/A^{\frac{1}{2}K}$.

First-order inner equations:

$$\rho_{i1}u_{i1} - (\rho_{i1}v_{i1})' = 0, \tag{A 6a}$$

$$u''_{i1} + \rho_{i1}v_{i1}u'_{i1} - [\rho_{i1}u^2_{i1}/(j+1)] + [\rho_0/(j+1)] = 0, \tag{A 6b}$$

$$p_{i1} = \text{constant}, \tag{A 6c}$$

$$h''_{i1} + \rho_{i1}v_{i1}h'_{i1} = 0, \tag{A 6d}$$

$$\alpha''_{i1} + \rho_{i1}v_{i1}\alpha'_{i1} + \frac{\Gamma}{A\rho_d}\rho^3_{i1}\left(\frac{\alpha^*_{i1}}{1-\alpha^*_{i1}} + \alpha_{i1}\right)(\alpha^*_{i1} - \alpha_{i1}) = 0, \tag{A 6e}$$

$$p_{i1} = (1+\alpha_{i1})\rho_{i1}T_{i1}, \tag{A 6f}$$

$$h_{i1} = (4+\alpha_{i1})T_{i1} + \theta\alpha_{i1}, \tag{A 6g}$$

$$\frac{\alpha^{*2}_{i1}}{1-\alpha^*_{i1}} = \frac{\rho_d}{\rho_{i1}}\exp(-\theta/T_{i1}). \tag{A 6h}$$

First-order inner boundary conditions. At the wall ($\eta = 0$) $u_{i1} = v_{i1} = 0$, $T_{i1} = T_w =$ constant, and $\alpha_{i1} = \alpha^*_{i1}$ (catalytic wall) or $\alpha'_{i1} = 0$ (inert wall). Here the unknown quantities are u'_{i1}, h'_{i1}, and α'_{i1} (or α_{i1} for the inert wall). The far boundary conditions ($\eta \to \infty$) are obtained by matching to the outer flow and are $u_{i1} = 1$, $h_{i1} = h_0$, $\alpha_{i1} = \alpha^*_{i1}$. Matching also gives $p_{i1} = p_0$.

The first-order inner problem represents the conventional boundary layer. It is a non-linear boundary-value problem, and is solved by guessing the three unknown quantities at the wall until the far boundary conditions are satisfied at sufficiently large values of η.

Second-order inner equations:

$$\rho_{i1}u_{i2} + u_{i1}\rho_{i2} - (v_{i1}\rho_{i2} + \rho_{i1}v_{i2})' = 0, \tag{A 7a}$$

$$u''_{i2} + \rho_{i1}v_{i1}u'_{i2} - \frac{2}{j+1}\rho_{i1}u_{i1}u_{i2} + \rho_{i1}u'_{i1}v_{i2} + \left(v_{i1}u'_{i1} - \frac{u^2_{i1}}{j+1}\right)\rho_{i2} - \frac{2(j+1)}{A^2}p_{i22} = 0, \tag{A 7b}$$

$$p_{i2} = \text{constant}, \tag{A 7c}$$

$$h''_{i2} + \rho_{i1}v_{i1}h'_{i2} + v_{i1}h'_{i1}\rho_{i2} + \rho_{i1}h'_{i1}v_{i2} = 0, \tag{A 7d}$$

$$\alpha''_{i2} + \rho_{i1}v_{i1}\alpha'_{i1}\left(\frac{\rho_{i2}}{\rho_{i1}} + \frac{v_{i2}}{v_{i1}} + \frac{\alpha'_{i2}}{\alpha'_{i1}}\right) - (\alpha''_{i1} + \rho_{i1}v_{i1}\alpha'_{i1}) \times \left[\frac{\alpha^*_{i1} - \alpha_{i2}}{\alpha^*_{i1} - \alpha_{i1}} + 3\frac{\rho_{i2}}{\rho_{i1}} + \frac{\alpha^*_{i2} + (1-\alpha^*_{i1})^2\alpha_{i2}}{(1-\alpha^*_{i1})\alpha^*_{i1} + (1-\alpha^*_{i1})^2\alpha_{i1}}\right] = 0, \tag{A 7e}$$

$$\frac{p_{i2}}{p_{i1}} = \frac{\alpha_{i2}}{1+\alpha_{i1}} + \frac{T_{i2}}{T_{i1}} + \frac{\rho_{i2}}{\rho_{i1}}, \tag{A 7f}$$

$$h_{i2} = (T_{i1} + \theta)\alpha_{i2} + (4+\alpha_{i1})T_{i2}, \tag{A 7g}$$

$$\alpha^*_{i2} = \frac{\alpha^*_{i1}(1-\alpha^*_{i1})}{2-\alpha^*_{i1}}\left(\frac{\theta}{T_{i1}}\frac{T_{i2}}{T_{i1}} - \frac{\rho_{i2}}{\rho_{i1}}\right). \tag{A 7h}$$

Second-order inner boundary conditions: At the wall ($\eta = 0$)

$$u_{i2} = v_{i2} = T_{i2} = \alpha_{i2} = \alpha^*_{i2} = 0.$$

Here the unknowns are u'_{i2}, α'_{i2} and h'_{i2}. The far boundary conditions ($\eta \to \infty$) are obtained by matching to the outer solution. They are: $u_{i2} \sim (C_u/A)\,\eta^K$, $\alpha_{i2} \sim C_\alpha \eta^K$, $\rho_{i2} \sim C_\rho \eta^K$, $h_{i2} = 0$, where C_u, C_α, C_ρ, A, K are constants obtained from the first-order outer solution. Matching also gives $p_{i2} = p_{i22} = 0$.

The second-order inner problem is linear, and therefore the solution is constructed by superposition of three solutions, where the unknowns at $\eta = 0$ are assigned arbitrarily. Then a linear combination of these solutions is formed in such a way as to satisfy the far boundary conditions at sufficiently large values of η.

The choice of co-ordinate system

The present problem poses conflicting requirements for the co-ordinate system. The outer solution should be carried out in shock-oriented co-ordinates, but the inner solution should be carried out in body-oriented co-ordinates. As a compromise we adopt the Cartesian system of figure 1, which, if less than ideal, is sufficient for present purposes. The outer problem is poorly posed in these co-ordinates, but we take advantage of the truncation assumption to improve the situation. We assign the value of p_{12} in such a way that the differential equations take on the form that would be obtained in polar co-ordinates centred on the centre of curvature of the shock wave; these are natural co-ordinates for the outer problem. In the first-order inner problem our Cartesian system is indistinguishable from the conventional 'boundary-layer' co-ordinates. It turns out that this is also true to second order, because the conventional effects of nose curvature, which are of relative order $R^{-\frac{1}{2}}$, are presently of a higher order than the second. However, we keep in mind that when the reaction parameter K exceeds unity, the conventional second-order effects take precedence, and the Cartesian system should be abandoned since it is inadequate to deal with the effects of nose curvature.

REFERENCES

BURGGRAF, O. R. 1966 Asymptotic solution for the viscous radiating shock layer. *A.I.A.A. J.* **4**, 1725.

CONTI, R. & VAN DYKE, M. 1969 Inviscid reacting flow near a stagnation point. *J. Fluid Mech.* **35**, 799.

HERSH, A. S. 1968 Ph.D. thesis, University of California at Los Angeles.

LEE, R. S. & CHENG, H. K. 1969 On the outer-edge problem of a hypersonic boundary layer. *J. Fluid Mech.* **38**, 161.

LIGHTHILL, M. J. 1957 Dynamics of a dissociating gas. Part 1. *J. Fluid Mech.* **2**, 1.

VAN DYKE, M. 1964 *Perturbation Methods in Fluid Mechanics*. New York: Academic Press.